



HAL
open science

Development and tribological characterisation of nanostructured Zn-Ni and Zn-Co coatings: a comparative study

Faten Narsi, Manel Zouari, Mohamed Kharrat, Maher Dammak, Florence Vacandio, Marielle Eyraud

► To cite this version:

Faten Narsi, Manel Zouari, Mohamed Kharrat, Maher Dammak, Florence Vacandio, et al.. Development and tribological characterisation of nanostructured Zn-Ni and Zn-Co coatings: a comparative study. Transactions of the Institute of Metal Finishing, 2018, 96 (4), pp.220-227. 10.1080/00202967.2018.1494876 . hal-02461507

HAL Id: hal-02461507

<https://hal.science/hal-02461507v1>

Submitted on 6 Feb 2020

HAL is a multi-disciplinary open access archive for the deposit and dissemination of scientific research documents, whether they are published or not. The documents may come from teaching and research institutions in France or abroad, or from public or private research centers.

L'archive ouverte pluridisciplinaire **HAL**, est destinée au dépôt et à la diffusion de documents scientifiques de niveau recherche, publiés ou non, émanant des établissements d'enseignement et de recherche français ou étrangers, des laboratoires publics ou privés.

Development and tribological characterization of nanostructured Zn-Ni and Zn-Co coatings: A comparative study.

Faten Nasri ^a, Manel Zouari ^a, Mohamed Kharrat ^{a*}, Maher Dammak ^a, Florence Vacandio ^b,
Marielle Eyraud ^b

^a Laboratory of electromechanical systems (LASEM), National Engineering School of Sfax, University of Sfax, Sfax, Tunisia

^b Aix Marseille Univ, CNRS, Madirel, UMR 7246, Electrochemistry of Materials Group, Campus St Jérôme, 13397 Marseille, France

* Correspondence should be addressed to:

Laboratory of electromechanical systems, National Engineering School of Sfax, Soukra Road, Km 3.5,

PO Box 1173, 3038 Sfax, Tunisia

Email: mohamed.kharrat@ipeis.rnu.tn

Fax: (+216) 74 246 347

Development and tribological characterization of nanostructured Zn-Ni and Zn-Co coatings: A comparative study.

Abstract

Zn-Ni and Zn-Co alloy coatings were electrodeposited on mild steel from sulfate-based baths. Morphology, microstructure, microhardness and tribological behaviors of the coatings have been studied and discussed. While the Zn-5wt% Co layers presented a simple nanocrystalline nodular structure (45 ± 5 nm), the Zn-14wt% Ni showed a cauliflower morphology (30 ± 7 nm). The X-ray diffraction analysis showed that both electrodeposits was formed by a mixture of hexagonal zinc phase and an intermetallic compound of γ_2 -phase (CoZn_{13}) for the Zn-5wt% Co alloy and γ -phase ($\text{Ni}_5\text{Zn}_{21}$) for the Zn-14wt% Ni alloys. The Zn-14wt% Ni films were found harder and rougher than the Zn-5wt% Co layers. Plastic deformation and oxide layers production were the main wear mechanisms for the investigated coatings. The Zn-14wt% Ni coatings presented the best wear resistance thanks to their microhardness and particular structure.

Keywords: Intermetallic Zn alloy coatings; Nanocrystalline Microstructure; Friction and wear behaviors.

1. Introduction

One of the effective solutions to improve the corrosion properties of zinc deposits is alloying Zn with an element of the iron group (Co, Ni, Mn, Fe).¹⁻⁶ In fact, Zinc-iron group alloys coatings have found practical applications, especially in the automotive industry.^{7,8} Currently, Zn-Co alloy coatings have drawn much attention thanks to their significant resistance corrosion compared to pure zinc coatings.⁹ Therefore, many research works have explored the plating of these coatings and their properties such as corrosion resistance, tribological behavior etc. Previously, a great deal of research focused on Zn-Co alloys with low Co content (< 3 wt. %) to improve the anticorrosive performances of the uncoated substrates. Actually, the quality of these coatings is influenced by different parameters such as bath composition, current density etc. These parameters were determined for the purpose of obtaining coatings with a fine morphology (320 nm, 200 nm...) and a single phase structure.¹⁰⁻¹⁴ The fine morphology and the single-phase structure were found to improve the micromechanical properties and the corrosion resistance of these coatings. Recently, other research works have attempted to prove that even Co-rich Zn-Co deposits are able to enhance the Zn-Co coatings' properties. This idea emanates from the fact that finer grains improved the anticorrosive properties.^{8,15-18} Acting as barrier coatings on steel substrates, the Zn-Co coatings with high Co content showed better anticorrosive performance than Zn-Co coatings with low Co content.¹⁹ Nevertheless, the coatings' performance with very high cobalt contents (e.g. 92 or 97 wt. %)^{15,16} were not found to provide adequate protection to the substrate.

The interest given in Zn-Co coatings' plating and corrosion resistance stability is followed by a very limited investigation of their tribological and mechanical behaviors. The wear behavior of Zn-Co electrodeposited coatings on copper substrates was investigated by Panagopoulos et

al.²⁰ The Zn-4wt% Co alloys' main wear mechanism found was a surface delamination mechanism. This study is being pursued by Panagopoulos et al.² to investigate the microhardness and the adhesion behavior of Zn-4.5 wt. % Co electrodeposits on mild steel with different thicknesses. They showed that the adhesive load of the Zn-Co coatings, with a single intermetallic phase γ_2 (CoZn_{13}), to the mild steel substrate decreased with the increase in coating thickness. This is due to the increase of residual stress in these coatings.

As another example of Zn-iron group alloys, the Zn-Ni alloy coatings have attracted much attention as Zn-Co coatings due to their similar improvement in corrosion resistance. For Zn-Ni coatings, the novelties tend to determine the best conditions used to improve their corrosion resistance. They found that the main parameters influencing the electrodeposition of these coatings are the bath composition and the density of the current. These parameters have been determined to obtain nanocrystalline Zn-Ni coatings with single-phase structure²¹⁻²⁴. In fact, the nanocrystalline Zn-Ni coatings with $\text{Ni}_5\text{Zn}_{21}$ as single-phase structure has proven the best corrosion protection performance. Along with the corrosion resistance, the mechanical and tribological behaviors of Zn-Ni alloys were studied. Actually, some investigations focused on the Ni content effect on the tribological behavior of these coatings²⁵. They found that the Zn-14wt % Ni alloys presented the lowest wear loss and friction coefficient. Furthermore, other studies showed that the main wear mechanism of Zn-14 wt% Ni coatings changed from a surface delamination to severe shearing by changing the counterpart material²⁶.

In the present study, simple sulfate baths with well-determined current densities were used to elaborate nanocrystalline Zn-Co and Zn-Ni coatings having almost the same grain size. The aim of this work is to investigate the tribological behavior of the nanocrystalline Zn-5wt% Co alloys coatings deposited on mild steel. Moreover, these coatings would be compared with the Zn-14wt% Ni layers in terms of micromechanical properties and tribological behavior.

2. Materials and methods

2.1. Electrodeposition process

The substrate material used in this study was mild steel. All specimens were machined to the dimensions of $30 \times 1.5 \times 2 \text{ cm}^3$. The chemical composition of the substrate was as follows: 0.17% C, 1.4% Mn, 0.045% S, 0.045% P and 98.34% Fe. The mild steel specimens were mechanically polished with 180, 400 and 1000 grit SiC paper. Only one side with 4.5 cm^2 as surface, was in contact with the electrolyte, while the back side was hidden with an insulating tape. The surface to be coated were activated in HCl and rinsed with dionized water and ethanol, prior to deposition.

The chemical composition of the electrolyte as well as the plating conditions are presented in Table 1. For both Zn-Co and Zn-Ni coatings, the mild steel substrate was used as a cathode and pure zinc specimen as an anode, in an electrochemical cell. After each Zn-Co and Zn-Ni electrodeposition, the coated steel specimens were rinsed in distilled water and ethanol. The thicknesses of both coating alloys were about $50 \text{ }\mu\text{m}$. The deposition time used to obtain this thickness was calculated by using Faraday's Law (equation (1)). The current densities used in this study were interpreted previously from cyclo-voltammetric and potentiostatic studies in sulfate baths. Then, after deposition, the intended thicknesses were confirmed by making an optical measurement of a cross-section of the coated substrates (Figure 1) after chemical etching (CrO_3 (20 g) and Na_2SO_4 (1.5 g) in 100 mL of distilled water) in order to increase substrate/coating contrast. After electrodeposition, the surface roughness of all samples was measured via a tactile profilometer. An average roughness of $1.4 \pm 0.2 \text{ }\mu\text{m}$ was detected in the case of Zn-Ni coating compared to the Zn-Co coating having more reduced surface roughness (average $0.5 \pm 0.1 \text{ }\mu\text{m}$).

$$e = \frac{M i t}{n F \rho} \quad (1)$$

With

i: Current density (A/cm²) F: Faraday constant: 96500 C/mol
t: Time (s) M: molar mass (g/mol)
e: thickness in cm ρ : density (g/cm³).

2.2. Structural characterization

The surface morphology of Zn-Co and Zn-Ni alloy coatings were examined with a Scanning Electron Microscope connected with an EDS facility (Philips XL30 ESEM, 20 KV). The crystallographic structure of the elaborated coatings was investigated using an X-ray diffractometer (XRD) Brucker–SIEMENS D5000 with Cu k_α radiation (λ=0.15440 nm) and a graphite monochromator.

The average crystallite size of the samples was calculated from the peak width at the half maximum of the peak (β), using the Debye–Scherrer equation²⁷:

$$D = \frac{0.9 \lambda}{\beta \cos \theta} \quad (2)$$

where λ is the wavelength of the X-ray radiation, θ is the Bragg angle of the peak, and β is the angular width of the peak at full-width at half maximum (FWHM).

2.3. Hardness and Tribological testing

The Vickers microhardness was measured under a load P of 1 daN for 14 s. The tests were developed using a diamond indenter in the shape of a square pyramid with an angle between edges α'=136°. For each test, the hardness H_v and the penetration h of the indenter were calculated from the measured value of the diagonal D footprint using the following expressions²⁸:

$$H_v = 1.854 \frac{P}{D^2} \quad (3)$$

$$h = \frac{D}{2 \operatorname{tg}\left(\frac{\alpha'}{2}\right)} \quad (4)$$

For the tribological characterization of zinc nickel coatings, a linear alternating motion tribometer was used. The sample was put in contact with a high chromium steel ball (100Cr6, 15 mm in diameter) under a constant normal load. The coated substrate was then driven in an alternating and translational movement produced by the combination of a gear motor and a rod/crank system. A force sensor was used to measure the tangential force and a data acquisition system allowed a continuous recording of this effort. The tests were developed for a frequency of 1 Hz, a displacement amplitude of ± 7.5 mm, a maximum cycles number of 5000 and an imposed normal force of 6 N, namely five tests were performed for each of the considered coating. At the end of each friction test, the data processing could be traced back to the changes in the friction coefficient evolution with the number of cycles.

Subsequently, the worn surface of the wear track was inspected with a Scanning Electron Microscope (Philips series XL30, 15 KV). Next, the wear track on the surface of the spherical antagonist is also observed by means of the optical microscope. At last, surface profile in the transverse direction across the wear scar on the coated specimen was established using a tactile profilometer "SJ-210". Based on this profile, the volume loss due to the wear was calculated.

3. Results and Discussion

3.1. Chemical composition and surface morphology of alloys coatings

Figure 2 shows the surface morphology of Zn-Co (a) and Zn-Ni (b) alloys coatings that mainly consist of a continuous and uniform surface with a nodular structure in both cases. For the Zn-Ni layers, the nodules were grouped together, forming clusters that leads to cauliflower

morphology. Using the EDS technique, the chemical composition of each coatings was found to be approximately Zn-5 wt% Co and Zn-14 wt% Ni.

3.2. Phase composition of the deposits

The X-ray diffraction patterns obtained from the electroplated Zn-Co and Zn-Ni alloy coatings are presented in Figure 3. The Zn-Co pattern reveals that this coating is a mixture of pure zinc with a hexagonal structure and an intermetallic γ_2 phase (CoZn_{13}) with a monoclinic structure. The last observation comes in full agreement with the Zn-Co phase diagram¹⁹. The presence of CoZn_{13} phase is also justified by the fact that the coatings contain a high Co content (5 wt %).^{29,30}

For the Zn-Ni alloy coatings, according to the figure 3, intermetallic compound was formed. The analysis of the different peaks showed that these coatings consisted of pure hexagonal zinc phase and a single γ -phase (intermetallic compound $\text{Ni}_5\text{Zn}_{21}$). This γ -phase presented a body centered cubic structure (bcc). This result agrees well with the Zn-Ni phase diagram³¹.

A small peak originated from the iron substrate is also performed.

The peaks coming from the pure zinc phase were less significant in Zn-14wt% Ni case. This is explained by the fact that the nickel percentage into the alloys is more important than that of the cobalt.

The average grain size of the coatings that were measured by Scherrer equation was calculated to be 45 ± 5 nm and 30 ± 7 nm for the Zn-Co and the Zn-Ni coatings, respectively.

3.3. Microhardness

The microhardness as well as the penetration depth of the Vickers indenter for both electrodeposited coatings are given in Table 2, from which it can be seen that Zn-Ni films are harder than Zn-Co layers. On one hand, this can be explained by the fact that the Ni content in

the Zn-Ni coating (14 wt%) is higher than that of the Co in the Zn-Co coating (5 wt%). On the other hand, metals electrodeposition from solution is escorted by the discharge of the hydrogen ions or water molecules^{32,33}. As previously mentioned, hydrogen release in Ni containing solution is very intense, and as a result, the hydrogen entrapped inside the coating might be more significant than that in Zn-Co. This phenomenon may generate intense internal stresses in the Zn-Ni coatings, and consequently work-hardening of it.

The Zn-Co layers deposited on mild steel substrates, in the present work, are harder than the Zn-Co films deposited on copper in the work of Panagopoulos et al.²⁰. This observation might be due to the susceptibility of the hard and brittle γ_2 intermetallic phase (CoZn_{13}) to be more concentrated by depositing on steel than on copper.

3.4. Tribological behavior

3.4.1. Friction behavior

During the sliding tests, the tangential force was measured and converted into a friction coefficient. The typical trends of the friction coefficient for both Zn alloy coatings when sliding against 100Cr6 counter-face are presented in Figure 4. For both electrodeposits, the friction coefficient increased rapidly during the first hundred cycles. It reached a maximum of 0.4 at 140 cycles for the Zn-Co layers, whereas, the maximum was about 0.45 at 100 cycles for the Zn-Ni films. This increase of the friction coefficient was followed by its decrease for both coatings. Then, for the Zn-Co coatings, the decrease of the coefficient continued until stabilization at 0.31. Thus, this experimental observation might be due to the establishment of a transfer film on the steel ball surface and a third body constituted of the detached particles on the coating wear track. Nevertheless, the Zn-Ni coatings, after the decrease of friction coefficient, showed a different friction response from that of Zn-Co coatings. Indeed, a reincrease in the friction coefficient was noted after about 350 cycles, which is a phenomenon

that could be explained by the transfer film loss. The hardened coating was found to be in direct contact with the counter-face and, consequently, the friction coefficient increased to 0.43 and then maintained this level to the end of the test. Therefore, after 5000 cycles, the friction coefficient of Zn-Co coatings was lower than that of the Zn-Ni coatings.

For comparable sliding conditions (6N normal load and spherical steel counter-face), the Zn-5wt% Co coatings electrodeposited on mild steel in the present work revealed a lower friction coefficient (0.31) than that (0.55) of the Zn-5wt% Co coatings electrodeposited on copper in the work of Panagopoulos et al.²⁰

3.4.2. Wear response

Figures 5 and 6 present the micrographs of the Zn-Co and Zn-Ni alloy coatings' wear track after 2500 and 5000 sliding cycles. These micrographs have proven that several mechanisms are in motion. For each of these cycle's numbers, the wear track width seems to be comparable for both coatings.

For the Zn-Co layers, after 2500 sliding cycles (Fig. 5.a), the wear scar showed much disruptions of the coating. Indeed, plowing phenomenon is located on the edges of the track, whereas, the track center reveals the presence of plastic deformation with the production of oxide layers. This observation is confirmed by zooming in the center of the wear track (Fig. 5.b). Indeed, the oxide layers and plastic deformation beginning of the Zn-Co alloy with a destruction of the coating structure are observed. By going further and after 5000 sliding cycles (Fig. 5.c), the same already observed mechanisms were in motion, but they are more developed. In fact, the center of the wear track (Fig. 5.d and e) presented a large plastic deformation with significant material wrenching scars. During the advancement of the wear test, coating's torn patches were re-deposited on the wear scar under plastic deformation. The coatings' torn patches were analyzed by XRD technique and the obtained pattern is shown in Figure 7.a. It can be seen that the wear particles were composed of pure Zn, intermetallic

phase CoZn_{13} , zinc oxide ZnO and cobalt oxide CoO . Fig. 8.a and b shows the optical micrographs of the wear scar on the steel ball antagonist, in the case of Zn-Co electrodeposit, after 2500 and 5000 sliding cycles. The scars on the counterface seem to be similar for both of cycles' number, yet after 5000 cycles, it is more significant. The wear scar on the ball surface is composed of plowing furrows, indicating that a hard abrasive wear mechanism is involved. The development of this mechanism is due to the increase of the detached particles hardness during the friction test. In fact, the detached particles become more and more oxidized and as a result, they can become harder than the steel ball antagonist itself. The presence of zinc oxide ZnO and mainly cobalt oxide CoO in the detached particles may confirm this wear mechanism.

For Zn-Ni coatings, the micrographs of the wear tracks after 2500 and 5000 cycles are shown in Figure 6. After 2500 cycles (Fig. 6.a), the plowing, plastic deformation and development of oxide layers were the principal wear mechanisms. A zoom on the worn surface center (Fig. 6.b) showed the presence of a plastic deformation with the entrapping of the detached particles between the valleys of the nodules forming an abraded cracked surface. The profile of the wear track appeared to be wavy due to the presence of the clusters. By increasing the sliding distance from 2500 cycles to 5000 cycles (Fig. 6.c), similar phenomena are observed, which are, however, more developed. For the wear track in this figure, two types of areas were observed: black areas and white areas. Black areas (Fig. 6.d) present plastic deformation with entrapped detached particles that are increasingly numerous by increasing the sliding distance. Nevertheless, white areas (Fig. 6.e) show the beginning of the coating structure destruction and particles entrapping. The presence of these two types of areas can be attributed to the presence of the clusters and the high roughness of the Zn-Ni coatings. The entrapment of debris in the coating wear track leads to the formation of a third body layer which becomes in a close contact with the antagonist steel ball after the removal of the

transfer film. The coatings' worn patches analysis by XRD technique (Fig. 7.b) showed that this debris was composed of pure Zn, intermetallic phase $\text{Ni}_5\text{Zn}_{21}$ and zinc oxide ZnO. Despite the presence of oxides in the wear track of the Zn-Ni coating, this presence was less significant than in the case of Zn-Co coating (Fig. 7.a). As a result, the interaction between the third body layer and the steel ball antagonist was expected to be relatively soft in the case of Zn-Ni coating. The optical micrographs of the wear scar on the steel ball antagonist for electrodeposit Zn-Ni after 2500 and 5000 sliding cycles are presented in Figure 8c and d. Indeed, by increasing the cycle's number from 2500 to 5000, the scars on the counter-face were more significant. Actually, the smooth track with some residues of transfer film was observed on steel ball surface for both numbers of cycles.

Figure 9 gives the topographic profiles of the various coatings' wear trace for 2500 and 5000 cycles. The different profiles take the form of an ellipse arc with a similar width for the different cycles' number and the different coatings: 1.15 mm for Zn-Ni layers and 1.5 mm for Zn-Co films. In terms of depth, the maximum depth became more significant from 2500 to 5000 cycles for both electrodeposits. However, according to Figure 9.c and mainly 9.d, it can be observed that the wear track of Zn-Ni coatings is not homogeneous (wavy), thus, there is a remarkable difference in depth throughout the track. This may confirm the microscopic observation of the wear track that has shown different areas due to the clusters presence. The wear volume loss for both electrodeposited coatings depending on the cycles' number was calculated and presented in Table 3. This table shows that the Zn-Co coatings surface has higher volume loss than that of the Zn-Ni alloys, for the different cycle's numbers, given their less significant microhardness and their weak grains cohesion. The wear volume loss was found to be slightly affected by the sliding distance, between 2500 and 5000 cycles, which is in agreement with the aforementioned conclusions from the analysis of the wear track micrographs. This result can be due to the entrapment of damaged debris within the contact

forming a third body that would prevent the direct interaction between the steel counterpart and the fresh coating surface toward the end of the test.

From the analysis of the wear mechanisms and volume losses, it appears clearly that the Zn-14wt% Ni alloy coatings have a better wear resistance than the Zn-5wt% Co alloy coatings.

4. Conclusion

The present study deals with the analysis of the friction and wear behavior as well as the morphological phase identification of electroplated Zn-Co and Zn-Ni coatings. Based on the tribological and morphological performances evaluation, the experimental findings led to the following conclusions:

- The surface roughness of Zinc-14wt%Ni coating was higher than that of Zinc-5wt% Co coating.
- Based on the Debye-Scherrer methods, it was found that the average grain size detected was nano-metric. Moreover, for Zinc-14wt%Ni, the particles size was smaller compared to Zinc-5wt% Co grain size.
- The Zinc-14wt%Ni coatings were harder than the Zinc-5wt% Co coatings.
- The stabilized friction coefficient of Zinc-5 wt% Co was found to be more reduced than that of Zinc-14wt%Ni.
- The main mechanisms of Zinc-5 wt% Co and Zinc-14wt%Ni wear were plowing, plastic deformation and development of oxide layers. The generation of oxides in the wear track was more significant in the case of Zn-Co coating involving a hard abrasive wear mechanism toward the end of the test. However, the interaction between the contacting bodies was relatively soft in the case of Zn-Ni coating.
- From the tribological analysis, we can deduce that the Zinc-5 wt% Co coating alloy have the higher friction ability compared to Zinc-14wt%Ni. Nonetheless, in terms of wear, it seems that Zinc-14wt%Ni coating alloy show better wear performance due to higher microhardness and particular structure.

Acknowledgement

The authors gratefully acknowledge the help and support of Professor Mongi Feki from the Laboratory of Materials Engineering and Environment (National Engineering School of Sfax; Sfax; Tunisia).

References

1. A. Marder : *Progr. Mater. Sci.*, 2000, **45**, 191.
2. C.N. Panagopoulos, D.A. Lagaris and P.C. Vatista: *Mater. Chem. Phys.*, 2011, **126**, 398.
3. N. Boshkov: *Electrochim. Acta.*, 2005, **51**, 77.
4. R. Fratesi, G. Roventi, G. Giuliani and CR. Tomachuk: *J. Appl. Electrochem.*, 1997, **27**, 1088.
5. I. H. Karahan and H.S. Guder: *Trans. Inst. Met. Finish.*, 2009, **87**, 155.
6. D.E. Hall: *Plat. Surf. Finish*, 1983, **70**, 59.
7. J. R. Garcia, D. C. B. do Lago and L.F. Senna: *Mater. Res.*, 2014, **17**, 947.
8. I. H. Karahan, O. Karabulut and U. Alver: *Phys.Scr.*, 2009, **79**, 5.
9. M. M. Abou-Krishna, F. H. Assaf and A. A. Toghian: *J. Solid State Electrochem.*, 1991, **11**, 692.
10. M. Heydari, M. H. Gharahcheshmeh and M. H. Sohi: *Mater. Chem. Phys.*, 2009, **117**, 414.
11. R. Ramanauskas, R. Juskenas, A. Kalinichenko and L. F. Garfias-Mesias: *J. Solid State Electrochem.*, 2004, **8**, 416.
12. J. B. Bajat, S. Stanković, B. M. Jokić and S. I. Stevanović: *Surf. Coat. Technol.*, 2010, **204**, 2745.
13. Z. I. Ortiz, P. Diaz-Arista, Y. Meas, R. Ortega-Borges and G. Trejo: *Corros. Sci.*, 2009, **51**, 2703.
14. S. Yogesha and A. Chitharanjan Hdge: *Bull. Mater. Sci.*, 2011, **34**, 1699.
15. S. Lichušina, A. Sudavičius, R. Juškenas, D. Bučinskiene and E. Juzeliūnas: *Trans. Inst. Met. Finish.*, 2008, **86**, 141.
16. J. R. Garcia, D. C. B. do Lago and L. F. Senna: *Mater. Res.*, 2014, **17**, 947.
17. Q. Chu, W. Wang, J. Liang, J. Hao and Z. Zhen: *Mater. Chem. Phys.*, 2013, **142**, 539.
18. J. R. Garcia, D. C. B. do Lago, D. V. Cesar and L. F. Senna: *Surf. Coat. Technol.*, 2016, 306, 462.
19. I. I. Kirilova, I. Ivanov and St. Rashkov: *J. Appl. Electrochem.*, 1997, **27**, 1380.

20. C. N. Panagopoulos, K. G. Georgarakis and S. Petroutzakou: *J. Mater. Process. Technol.*, 2005, **160**, 234.
21. A. Tozar and I. H. Karahan: *Appl. Surf. Sci.*, 2014, **318**, 15.
22. S. Ghaziof and W. Gao: *Appl. Surf. Sci.*, 2014, **311**, 635.
23. Z. Feng, Q. Li, J. Zhang, P. Yang, H. Song and M. An: *Surf. Coat. Technol.*, 2015, **270**, 56.
24. R. Ramanauskas, L. Gudavičiūtė, A. Kosenko, O. Girčienė and A. Selskis: *Trans. Inst. Met. Finish.*, 2013, **90**, 237.
25. M. Tafreshi, S. R. Allahkaram and H. Farhangi: *Mater. Chem. Phys.*, 2016, **183**, 263.
26. C. N. Panagopoulos, K. G. Georgarakis and P. E. Agathocleous: *Tribol. Int.*, 2006, **36**, 619.
27. M. M. Younan *Appl. Electrochem.* 2000, **30**, 55.
28. Caprentier L 1994 Ph D Thesis (Ecole Centrale de Lyon).
29. E. Gómez, X. Alcobe and E. Vallés: *J. Electroanal. Chem.*, 2001, **505**, 54.
30. A. E. Mohamed, S. M. Rashwan, S. M. Abdel-Wahaab and M. M. Kamel: *J. Appl. Electrochem.*, 2003, **33**, 1085.
31. X. Su, N. Y. Tang and J. M. Toguri: *J. Phase Equilibria*, 2002, **23** (2), 140.
32. M. A. V. Devanathan, Z. Stachurski and W. Beck: *J. Electrochem. Soc.*, 1964, **111**, 619.
33. J. O'M. Bockris and D. F. A. Koch: *J. Phys. Chem.*, 1961, **65**, 1941.

Figure captions

Fig. 1: Optical micrographs of the coatings' cross section: a) Zn-Co and b) Zn- Ni.

Fig. 2: SEM micrographs of electrodeposited Zn-5wt% Co (a) and Zn-14wt% Ni (b) alloy coatings.

Fig. 3: X-ray diffraction patterns of Zn-14wt% Ni and Zn-5wt% Co coatings.

Fig. 4: Friction coefficient evolution versus sliding cycle's number for Zn-5wt% Co and Zn-14wt% Ni alloy coatings.

Fig. 5: SEM wear track morphologies of Zn-5wt% Co alloy coating after 2500 (a, b) and 5000 sliding cycles: (c, d, and e).

Fig. 6: SEM wear track morphologies of Zn-14wt% Ni alloy coating after 2500 (a, b) and 5000 sliding cycles: (c, d, and e).

Fig. 7: X-ray diffraction patterns of Zn-5wt% Co (a) and Zn-14wt% Ni (b) coatings' torn patches after 5000 cycles.

Fig. 8: Optical micrographs of the wear scar on the steel ball antagonist for the Zn-5wt% Co alloy coating (a: 2500 cycles, b: 5000 cycles) and the Zn-14wt% Ni alloy coating (c: 2500 cycles, d: 5000 cycles).

Fig. 9: Wear track profiles of Zn-Co (a, b) and Zn-Ni (c, d) coatings after 2500 and 5000 cycles.

Table captions

Table 1: Sulfate baths used for the electroplating of Zn-Co and Zn-Ni alloy coatings on mild steel.

Table 2: Microhardness and penetration depth of the Vickers indenter for Zn-5wt% Co and Zn-14wt% Ni electrodeposits.

Table 3: Wear volume loss of Zn-Co and Zn-Ni coatings after 2500 and 5000 sliding cycles.

Figure 1

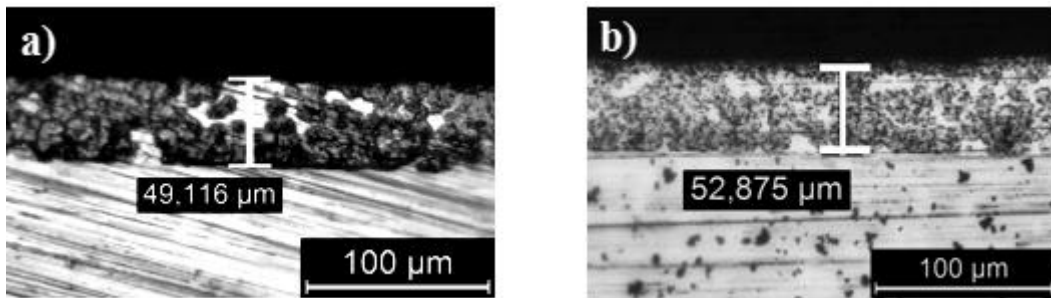


Figure 2

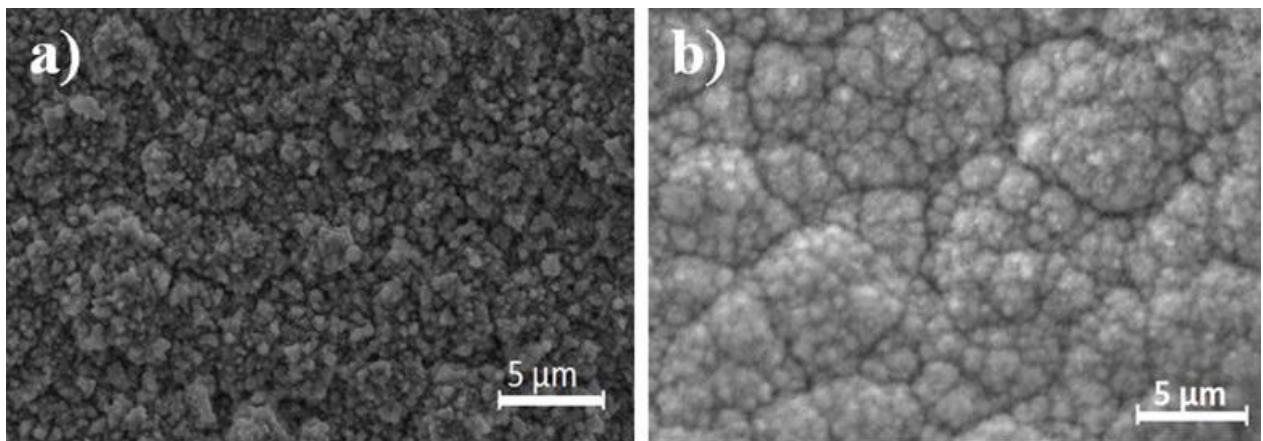


Figure 3

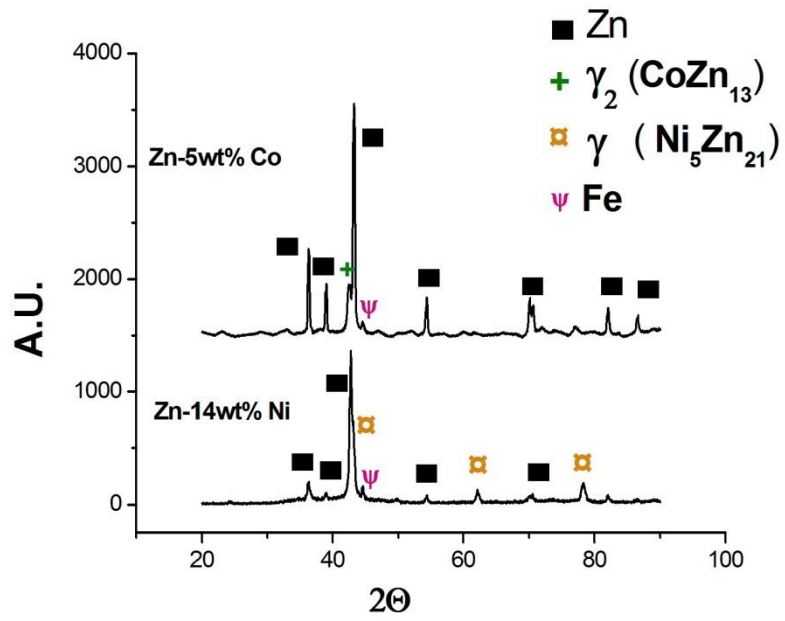


Figure 4

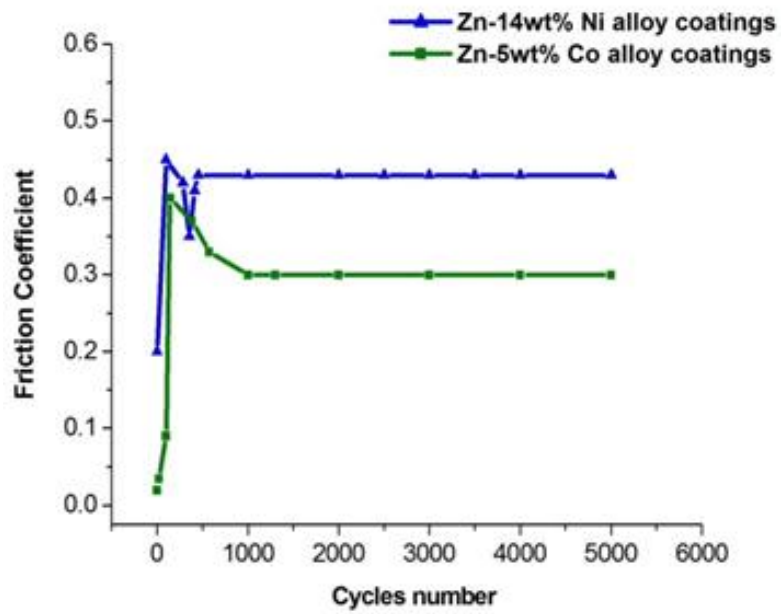


Figure 5

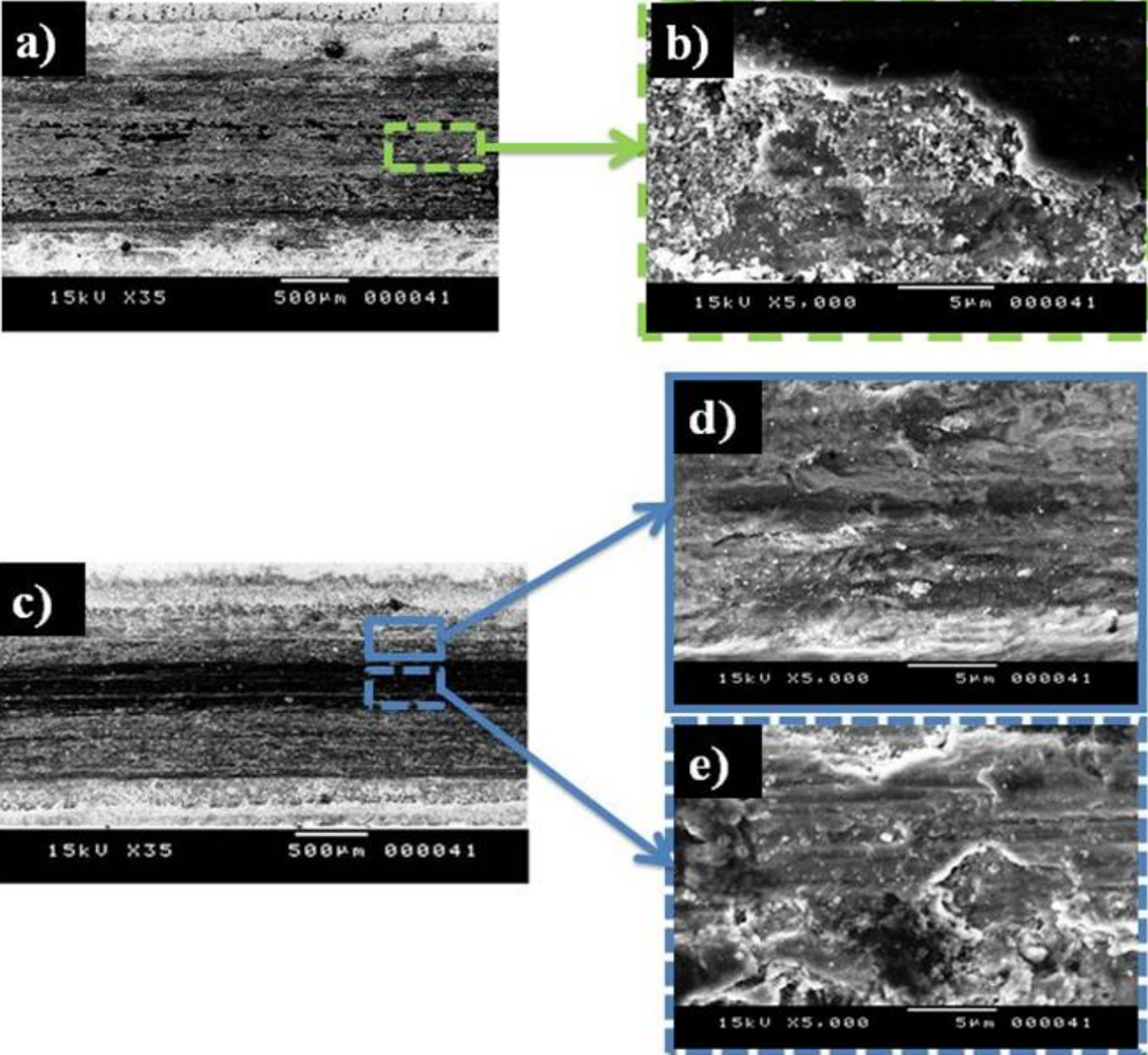


Figure 6

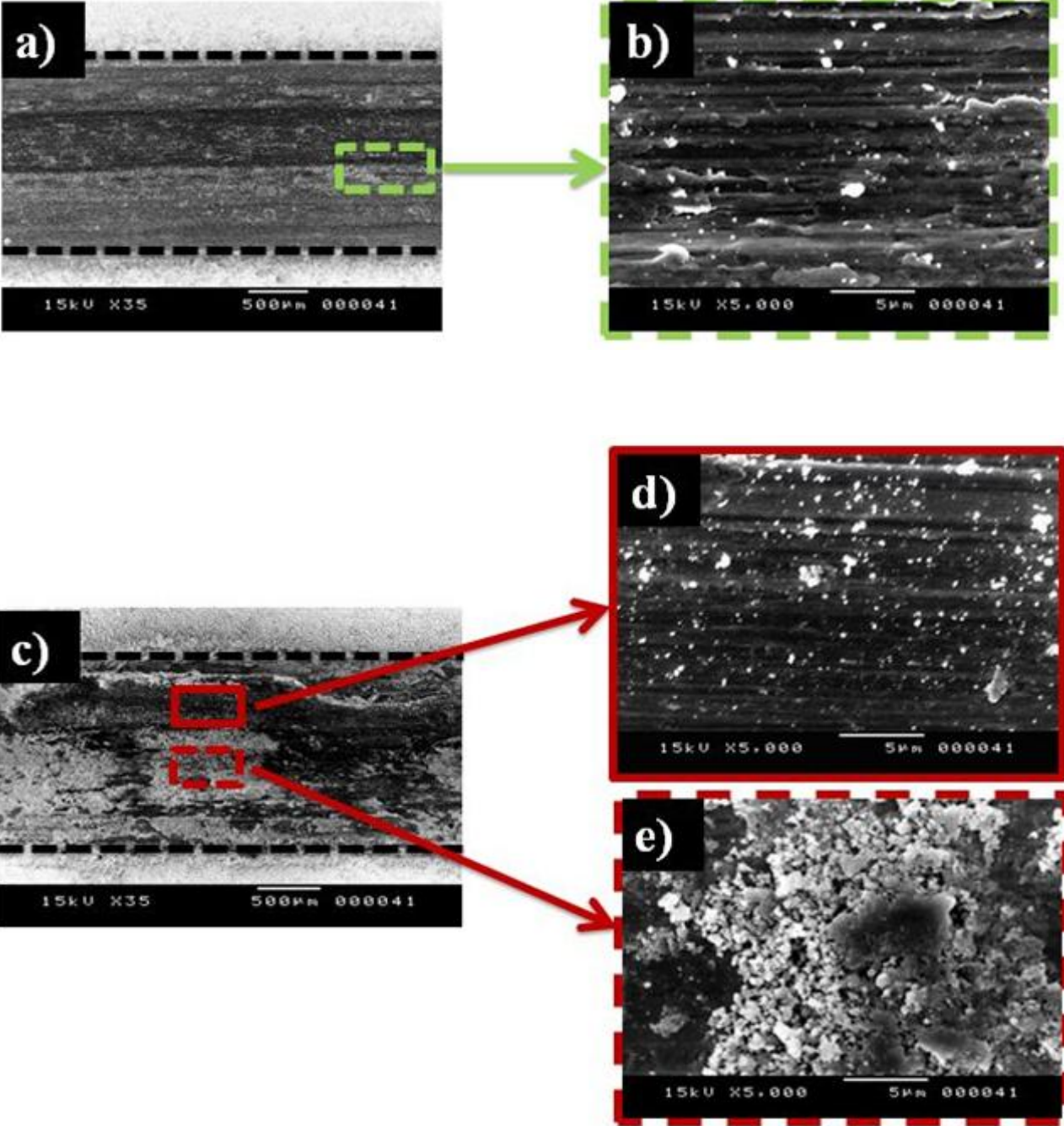


Figure 7

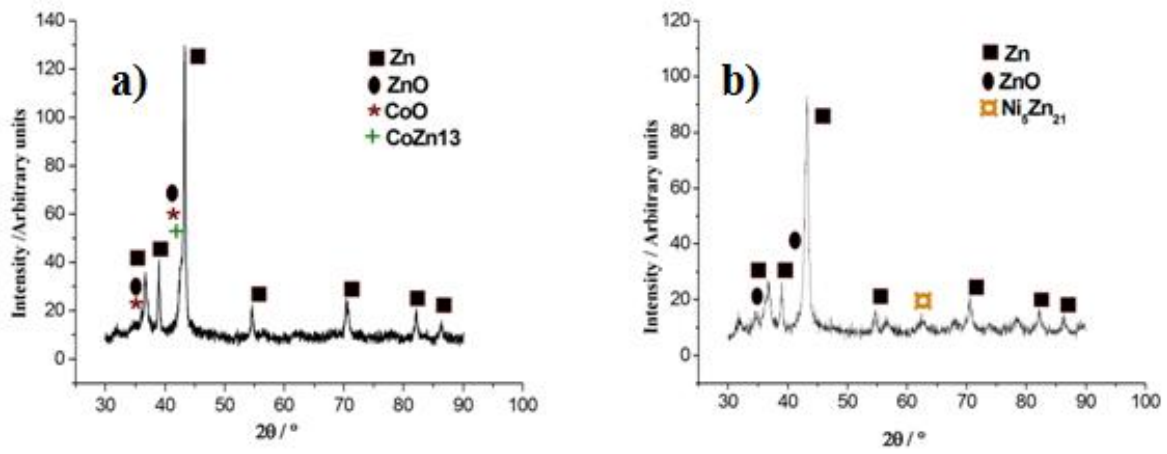


Figure 8

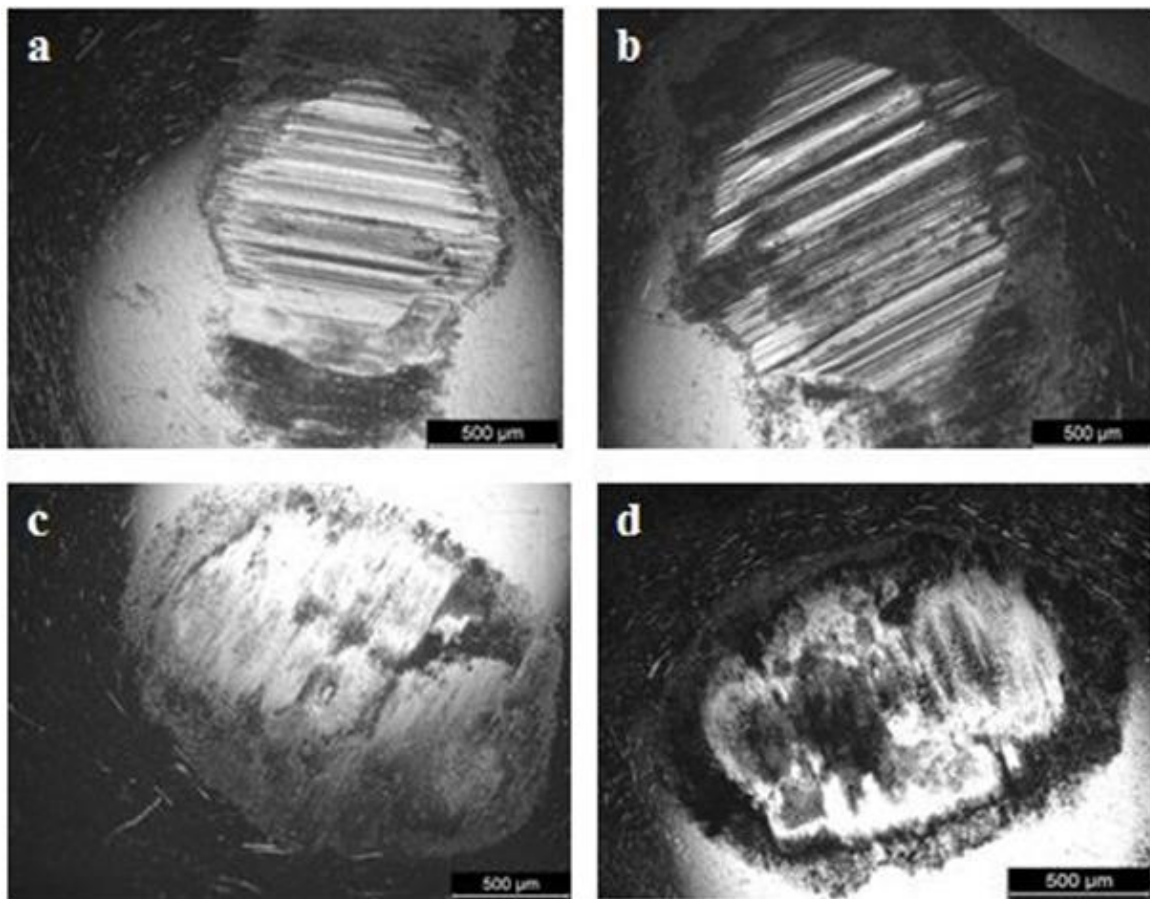


Figure 9

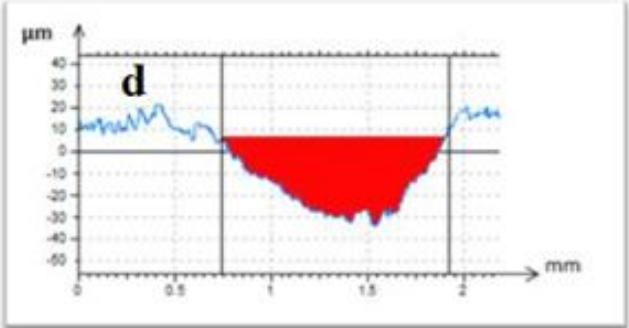
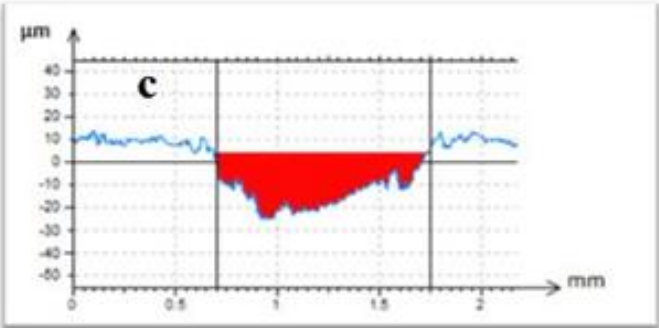
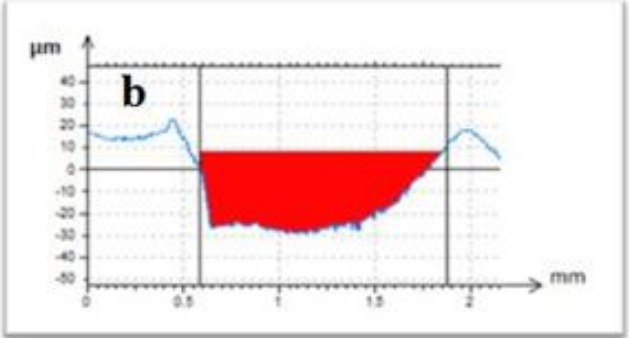
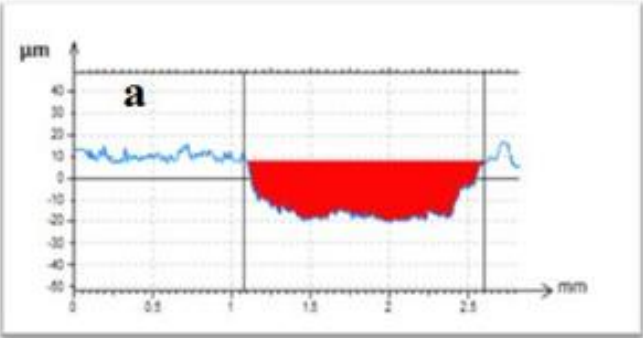


Table 1

Coatings	Zn-Co	Zn-Ni		Zn-Co	Zn-Ni
Bath composition (g/l)			Operating conditions		
ZnSO ₄ .7H ₂ O	150	347.5	Temperature (°C)	24	60
CoSO ₄ .7H ₂ O	372	-	PH	1.7	1-2
Na ₂ SO ₄	33	-	Current density (A/dm ²)	2	4.2
NiSO ₄ .6 H ₂ O	-	44.75	Plating time (min)	90	80
SnSO ₄	-	0.01	Electrolyte volume (ml)	250	250
			Anode	Zinc	Zinc
			Cathode	Mild steel	Mild steel

Table 2

	Medium Penetration h (μm)	Microhardness (Hv)
Zn-5wt% Co	3	123±4
Zn-14wt% Ni	2.5	233.5±12

Table 3

	Wear volume loss (mm ³)	
	2500 cycles	5000 cycles
Zn-5wt% Co	0.51±0.015	0.58±0.3
Zn-14wt% Ni	0.33±0.03	0.43±0.4